Identification of relaxation mechanisms in nonlinear spectroscopy of electron resonances of semiconductors

V. M. Petnikova, S. A. Pleshanov, and V. V. Shuvalov

Moscow State University
(Submitted 3 May 1984)
Zh. Eksp. Teor. Fiz. **88**, 360–371 (February 1985)

We report effective use of a new method of investigating subpicosecond processes in semiconductors. The method is based on the optical nonlinearity of one-photon electronic transitions. The times of a number of elastic and inelastic processes in gallium selenide were measured within the framework of the model constructed. The good agreement of the experimental results demonstrates the applicability of the phenomenological approach to a number of problems of nonlinear spectroscopy of condensed media.

1. INTRODUCTION

Relaxation time is determined in modern nonlinear spectroscopy by two methods. The probing-beam method (time analysis) proposes the use of light pulses shorter than the relaxation times.[1–4] More promising for the investigation of rapid processes is therefore the use of parameteric interaction of either fields with different frequencies (biharmonic pumping—spectral analysis),[5,7] or of noise radiation with a short correlation time.[8] The time scale of the investigated phenomena is set by the period of the beats or by the field-correlation time.

The nonlinear response of a semiconductor is determined by various types of inhomogeneities and by their relaxation mechanisms. Foremost is the presence of a band structure, i.e., the spectral inhomogeneous broadening of the electronic transition. The interaction of the field with matter is subject also to polarization inhomogeneity that upsets the equilibrium distribution of the electron-quasimomentum orientations. The spatial inhomogeneity of the light field brings about one more type of inhomogeneity, viz., irregular distribution of the excitation. The objective difficulty in the investigation is that in each particular experiment it is impossible to separate any one of the many types of relaxation mechanism. On the other hand, the experimental data are frequently set in correspondence, without due justification, with very simple models of one selected process or another.[1–3,5–11]

We report here effective use, in subpicosecond spectroscopy of parametric processes in semiconductors, of parametric processes with cubic nonlinearity of the one-photon electronic transitions. When a substance is acted upon by three fields with amplitudes $\mathbf{E}_{1-3}$ and frequencies ω_{1-3} close to the resonant transition frequency ω_0, and wave vectors $\mathbf{k}_{1-3}$, a fourth wave $\mathbf{E}_4$ is generated, of frequency $\omega_4 = \omega_1 + \omega_2 + \omega_3$, in the direction $\mathbf{k}_4 = \mathbf{k}_1 + \mathbf{k}_2 + \mathbf{k}_3$. The advantage of the method lies in the absence of a background in the latter direction. Investigation of the dependence of the effectiveness of the process on the various parameters makes it possible to identify the relaxation mechanisms of the medium. A set of experiments aimed at measuring and identifying the relaxation times was organized on the basis of a nonlinear susceptibility model constucted in this paper, in which account is taken of the main types of the relaxation of free carriers in energy, quasimomentum, and space.

2. MODEL KINETIC EQUATIONS

We develop here a phenomenological approach based on the kinetic equations (KE) given in Ref. 12 for the density matrix. The specific formulation of the KE is based on models that represent the relaxation processes (Fig. 1). These will be assumed hereafter to be Markov processes, and the deviations from the equilibrium states will be assumed small. This assumption can be justified in the cases of sufficiently long light pulses, of high equilibrium population of the upper level, and of weak excitation.[12] The fact that the relaxation processes are not of the Markov type alters substantially the character of the nonlinear response of the medium.[10,11]

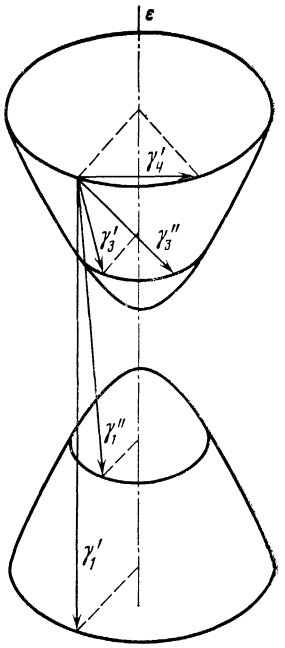

FIG. 1. Scheme of interband and intraband relaxation processes in a semiconductor.

 0038-5646/85/020211-07$04.00

The assumption that the perturbation is small is natural, since the end purpose of this paper is the determination of the rates of relaxation processes that are not distorted by the measurement procedure. The coefficients of the relaxation matrix are independent in this case of the time and satisfy the detailed-balancing principle.[12]

The internal state of the model medium is characterized by an electron quantum number ($i = 1, 2$ for the valence and conduction bands), by the electron energy ε_i reckoned from the bottom of the conduction band, by the orientation of the dipole moment $\boldsymbol{\mu}(\boldsymbol{\theta} = (\theta, \varphi))$ or of the electron quasimomentum parallel to it,[13] and by the spatial coordinate $\mathbf{r}$. The last three quantities are assumed continuous and are determined by distribution functions $f(a)$ ($a = (\varepsilon_{1,2}\ \boldsymbol{\theta}, \mathbf{r})$). The intraband evolution of the system is thus described classically.[13]

The relaxation mechanisms mentioned are assumed independent, and are described by combinations of three possible collision-integral types: I—$\varphi(a, a') = f_0(a)$; II—$\varphi(a, a') = \delta(a - a')$; III—diffusive relaxation process. Here $f_0(a)$ is the equilibrium distribution function and $\delta(a - a')$ is a delta function.

The relaxation processes in a semiconductor are divided into two groups (Fig. 1)—interband and intraband. It is assumed hereafter that a transition from the conduction to the valence band can occur either with satisfaction of the energy selection rules (direct transitions) or without but with the remaining parameters ($\boldsymbol{\theta}$, $\mathbf{r}$) conserved. The rates of the interband transitions are designated γ and γ', respectively. The rate of the inverse transition is assumed much lower.

The following processes are allowed in intraband transitions:

1. Inelastic relaxation, with and without rotation of the dipole moment, at rates γ_3'' and γ_3'.

2. Elastic relaxation the quasimomentum orientation, taking place both at a rate γ_4' and with a diffusion coefficient D_θ.

3. All the preceding processes were assumed localized in space. We consider in addition elastic relaxation in which the dipole moment and spatial diffusion of the carriers are preserved; it has a diffusion coefficient D_r.

The transverse relaxation rate γ_2 is also assumed constant and is determined by the sum of the rates of all the relaxation processes. The equilibrium distribution functions are assumed to be rectangular and the same for both bands, and the medium is assumed isotropic ($f_0(\boldsymbol{\theta}) = \frac{1}{4}\pi$).

When a KE model is devised for a direct-band semiconductor it is natural to assume that in field-induced optical transitions the values of $\boldsymbol{\theta}$ and $\mathbf{r}$ are preserved and that the selection rules hold for the electron energy number ($\varepsilon_2 = -\varepsilon_1$). The KE take now the form

$$\frac{\partial \sigma_1}{\partial t} = \frac{2\,\mathrm{Im}\, V\sigma_{21}}{\hbar} + \gamma_1'\sigma_2 - \gamma_1''f_0(\varepsilon)\int \sigma_2 d\varepsilon - \gamma_3\left[\sigma_1 - f_0(\varepsilon)\int \sigma_1 d\varepsilon\right] - \gamma_3''\left[\sigma_1 - f_0(\varepsilon)f_0(\theta)\int \sigma_1\, d\varepsilon\, d\theta\right] - \gamma_4'\left[\sigma_1 - f_0(\theta)\int \sigma_1 d\theta\right] + D_\theta \nabla_\theta^2 \sigma_1 + D_r \nabla_r^2 \sigma_1, \tag{1a}$$

$$\frac{\partial \sigma_2}{\partial t} = \frac{-2\,\mathrm{Im}\, V\sigma_{21}}{\hbar} - (\gamma_1' + \gamma_1'')\sigma_2 - \gamma_3'\left[\sigma_2 - f_0(\varepsilon)\int \sigma_2 d\varepsilon\right] - \gamma_3''\left[\sigma_2 - f_0(\varepsilon)f_0(\theta)\int \sigma_2 d\varepsilon d\theta\right] - \gamma_4'\left[\sigma_2 - f_0(\theta)\int \sigma_2 d\theta\right] + D_\theta \nabla_\theta^2 \sigma_2 + D_r \nabla_r^2 \sigma_2, \tag{1b}$$

$$\frac{\partial \sigma_{21}}{\partial t} = -\frac{i}{\hbar} V(\sigma_1 - \sigma_2) - \sigma_{21}\left[\gamma_2 + i\left(\omega_0 + \frac{2\varepsilon}{\hbar}\right)\right]. \tag{1c}$$

Here $\sigma_i = \sigma_{i\varepsilon,i\varepsilon}(\boldsymbol{\theta}, \mathbf{r})$, $\sigma_{ij} = \sigma_{i\varepsilon,j\varepsilon}(\boldsymbol{\theta}, \mathbf{r})$ are the density-matrix elements,

$$V = V_{1\varepsilon,2\varepsilon} = -\frac{\mu}{2}\sum_{i=1}^{3} \mathbf{E}_i \exp\{-i(\omega_i t - \mathbf{k}_i \mathbf{r})\} + \text{c.c.}$$

is the interaction Hamiltonian in the dipole approximation, and $\hbar\omega_0$ is the band gap,

$$\nabla_\theta^2 = \frac{1}{\sin\theta}\frac{\partial}{\partial\theta}\left(\sin\theta\frac{\partial}{\partial\theta}\right) + \frac{1}{\sin^2\theta}\frac{\partial^2}{\partial\varphi^2},$$

$$\nabla_r^2 = \frac{\partial^2}{\partial x^2} + \frac{\partial^2}{\partial y^2} + \frac{\partial^2}{\partial z^2}.$$

3. NONLINEAR POLARIZATION AND SCATTERED FIELD

The self-consistent problem was determined by the constructed KE (1) and by the abbreviated equations for the field amplitudes.[14] The z axis was perpendicular to a plane nonlinear layer of thickness l. The problem was solved for the frequency and spatial [$\boldsymbol{\varkappa} = (k_x, k_y)$] Fourier components of the density matrix by successive approximations, a method justified by the assumption that the perturbation is weak. By determining the linear polarization we could find the absorption coefficient of the medium in the linear approximation, $s_i = 2\pi\omega_i\mu^2 N/3\hbar c\gamma_2^*$. Here N is the particle density, $\gamma_2^* = 2\Delta\varepsilon/\pi\hbar$ the inhomogeneous width of the transition, and $2\Delta\varepsilon$ the width of the distribution $f_0(\varepsilon)$. It was assumed that γ_2^* exceeds all the relaxation rates and the optical-excitation detunings $|\omega_i - \omega_j|$; $i, j = 1$–4.

To determine the nonlinear polarization at the required frequency ω_4, equations were written and the following values obtained:

$$\iint \sigma_k(\omega_i - \omega_3)\, d\varepsilon\, d\theta, \quad \iint \mu_\alpha\mu_\beta\sigma_k(\omega_i - \omega_3)\, d\varepsilon\, d\theta,$$

$$\iint \frac{\sigma_k(\omega_i - \omega_3)}{\gamma_2 + i(\omega_0 - \omega_1 - \omega_2 + \omega_3 + 2\varepsilon/\hbar)}\, d\varepsilon\, d\theta,$$

$$\iint \frac{\mu_\alpha\mu_\beta\sigma_k(\omega_i - \omega_3)}{\gamma_2 + i(\omega_0 - \omega_1 - \omega_2 + \omega_3 + 2\varepsilon/\hbar)}\, d\varepsilon\, d\theta,$$

$$i, k = 1, 2; \quad \alpha, \beta = x, y, z.$$

The spatial-diffusion boundary-value problem was solved with boundary conditions of the second kind corresponding to the absence of an excited-particle flux at the boundaries of the nonlinear layer. Solution of the standard abbreviated

equations with the obtained polarization yielded the scattered-field amplitude.

The general expression obtained for $\mathbf{E}_4$ is too unwieldy to write out here. It constitutes a set of Lorentz profiles whose widths are determined by combinations of the rates of the introduced relaxation processes. The tensor character of the nonlinear susceptibility is described by the quantities

$$Y_{\alpha\beta\xi\eta}=\frac{1}{4\pi\mu^4}\int \mu_\alpha\mu_\beta\mu_\xi\mu_\eta\, d\theta,$$

$$Y_{\alpha\beta}=\frac{1}{4\pi\mu^2}\int \mu_\alpha\mu_\beta\, d\theta; \quad \alpha,\beta,\xi,\eta=x,y,z.$$

The expressions for $\mathbf{E}_4$ are greatly simplified by a special choice of the interacting-wave polarizations. Let $\mathbf{e}_1=\mathbf{e}_2$, with $\mathbf{e}$ the polarization vector. For crossed polarizations we have then

$$\mathbf{e}_3\mathbf{e}_{1,2}=0, \quad \sum_{\alpha,\beta} Y_{\alpha\beta}e_{i\alpha+}e_{3\beta}=0,$$

$$E_{4\alpha}^{(\pi/2)}=\sum_{i\neq j=1,2}\sum_{n=0}^{\infty} C_{\alpha ij}^{(n)}E_i^0E_j^0E_3^{0*}\Big[\frac{1}{\gamma_1+\gamma_3'+\gamma_4+\gamma_{5j}+\gamma_{6n}+i\Delta\omega_j}$$
$$\times\Big(1-\frac{\gamma_1+\gamma_{5j}}{\gamma_3'+\gamma_4+\gamma_{6n}-i\Delta\omega_j}\Big)\Big(\frac{1}{2\gamma_2-i\Delta\omega}+\frac{\gamma_3'}{\gamma_2^*}$$
$$\times\frac{1}{\gamma_1+\gamma_4+\gamma_{5j}+\gamma_{6n}-i\Delta\omega_j}\Big)+\frac{1}{\gamma_3'+\gamma_4+\gamma_{6n}-i\Delta\omega_j} \qquad (2)$$
$$\times\Big(\frac{1}{2\gamma_2-i\Delta\omega}+\frac{\gamma_3'-\gamma_1''}{\gamma_2^*}\frac{1}{\gamma_1+\gamma_4+\gamma_{5j}+\gamma_{6n}-i\Delta\omega_j}\Big)\Big].$$

Here

$$\gamma_1=\gamma_1'+\gamma_1'', \quad \gamma_4=\gamma_4'+\gamma_3''+D_\theta/6, \quad \gamma_{5j}=D_r|\varkappa_j-\varkappa_3|^2,$$
$$\gamma_{6n}=(\pi n/l)^2D_r, \quad \Delta\omega_j=\omega_j-\omega_3, \quad \Delta\omega=\omega_1+\omega_2-2\omega_3,$$

$$C_{\alpha ij}^{(n)}=-\frac{\pi\omega_4\mu^4Ne^{-s_4l}}{c\hbar^3\gamma_2^*l(1+\delta_{0n})}\varphi(k_{iz}-k_{4z}, s_i-s_4)$$
$$\times\varphi(k_{jz}-k_{3z}, s_j+s_3)\sum_{\beta,\xi,\eta} Y_{\alpha\beta\xi\eta}e_{i\beta}e_{j\xi}e_{3\eta},$$

δ_{0n} is the Kronecker delta; $\mathbf{E}_i^0$ is the amplitude of the ith field at the entrance to the nonlinear medium, and

$$\varphi(x,y)=\frac{(ix-y)\,[1-(-1)^ne^{(ix-y)l}]}{(ix+y)^2-(\pi n/l)^2}.$$

As in organic dyes,[4] in isotropic media there is a definite angle between the polarizations, $(\mathbf{e}_3\mathbf{e}_{1,2})=\psi_0=\arctan\sqrt{2}$, such that

$$\sum_{\beta\xi\eta}(Y_{\alpha\beta\xi\eta}-Y_{\alpha\beta}Y_{\xi\eta})e_{i\beta}e_{j\xi}e_{3\eta}=0.$$

With this choice, the field amplitude $\mathbf{E}_4$ is independent of the times that govern the orientational relaxation. An expression for $\mathbf{E}_4^{(\psi_0)}$ can be obtained by making the substitutions $\gamma_4\to 0$, $\gamma_3'\to\gamma_3=\gamma_3'+\gamma_3''$.

In nonstationary problems it is necessary to know the time dependence of the scattered field. It is determined by a triple Fourier integral of Eq. (2):

$$E_{4\alpha}^{(\pi/2)}=\sum_{i\neq j=1,2}\sum_{n=0}^{\infty} C_{\alpha ij}^{(n)}\int_0^\infty d\tau_j\int_0^{\tau_f} d\tau_i E_i^0(t-\tau_i) \qquad (3)$$
$$\times E_j^0(t-\tau_j)E_3^{0*}(t-\tau_i-\tau_j)$$
$$\times\Big\{\Big[2+\frac{\gamma_1''}{\gamma_1+\gamma_{5j}}(\exp\tau_j(\gamma_1+\gamma_{5j})-1)\Big]\Big[1-\frac{\delta(\tau_i)}{\gamma_2^*}\Big]$$
$$+\frac{2\delta(\tau_i)}{\gamma_2^*}\exp(\tau_j\gamma_3')\Big\}$$
$$\times\exp[-2\gamma_2\tau_i-(\gamma_1+\gamma_3'+\gamma_4+\gamma_{5j}+\gamma_{6n})(\tau_j-\tau_i)].$$

The value of $\mathbf{E}_4^{(\psi_0)}$ can be obtained by making the same substitutions.[4]

4. IDENTIFICATION OF THE RELAXATION PROCESSES

Analysis of the foregoing results confirms the statement that it is difficult to distinguish between the relaxation processes. It is nevertheless possible to construct a measurement system that solves this problem.

Semiconducting materials are characterized by the existence of two substantially different groups of fast and slow relaxation mechanisms:

$$\gamma_2,\ \gamma_3',\ \gamma_3'',\ \gamma_4\gg\gamma_1',\ \gamma_1'',\ \gamma_{5j},\ \gamma_{6n}. \qquad (4)$$

The characteristic times are shorter than 1 ps for the fast processes and exceed 100 ps for the slow ones.[1,2,4,7,9,13] The optimal procedure for the measurement of both the fast and slow relaxation time can be taken to be a combination of the probing-pulse and biharmonic-pumping methods. Two tunable-frequency radiation sources must be used with an intermediate pulse duration $\tau_p\sim 10$ ps. One of them ensures operation of the apparatus in the required spectral band, and the fast times are measured by tuning the second.

The measurements in the group of slow times are based on the probing-pulse technique. The time-synchronized fields $\mathbf{E}_1$ and $\mathbf{E}_3$, with an angle ψ_0 between their polarizations, produce in the investigated medium a diffraction grating. The latter is sounded by the probing pulse $\mathbf{E}_2$, which is delayed by a time $t\sim\gamma_{\text{slow}}^{-1}\gg\tau_p$ relative to the fields $\mathbf{E}_{1,3}$. The expression for the scattered field is then greatly simplified. No diffraction grating is formed by the pulses $\mathbf{E}_{2,3}$ ($i=1$, $j=2$) that intersect in time; the rapidly decaying terms vanish:

$$E_{4\alpha}^{(\psi_0)}(\tau)\sim\sum_{n=0}^{\infty} C_{\alpha 21}^{(n)}\exp[-\tau(\gamma_1+\gamma_{51}+\gamma_{6n})]. \qquad (5)$$

The longitudinal relaxation (γ_1) and the transverse spatial diffusion (γ_{51}) are separated by a change of the angle between the incident interaction waves $\mathbf{E}_{1,3}$ and the ensuing change of the spatial-grating period. The spatial-diffusion coefficient D_r determined in this manner permits an estimate of the number of terms n in the sum (5) and yields the required times γ_{6n}^{-1}. It is impossible to distinguish between γ_1' and γ_1''.

The measurements in the group of fast times ($\gamma_{2,3,4}$) were by the method of biharmonic pumping, the latter effected by tuning the frequency of $\mathbf{E}_3$ and letting $\mathbf{E}_1 = \mathbf{E}_2$. The scattered field is in this case

$$E_{i\alpha}^{(\pi/2)} \sim \frac{1}{\gamma_3'+\gamma_4-i\Delta\omega_1}\left[\frac{1}{\gamma_2-i\Delta\omega_1}+\frac{2\gamma_3'}{\gamma_2^*}\frac{1}{\gamma_4-i\Delta\omega_1}\right],$$

$$E_{i\alpha}^{(\psi_0)} \sim \sum_{n=0}^{\infty}\frac{C_{\alpha 11}^{(n)}}{\gamma_3-i\Delta\omega_1}\left[\frac{1}{\gamma_2-i\Delta\omega_1}+\frac{2\gamma_3}{\gamma_2^*}\frac{1}{\gamma_1+\gamma_{51}+\gamma_{6n}-i\Delta\omega_1}\right]. \quad (6)$$

A procedure for determining the remaining unknown relaxation times will be described below.

5. EXPERIMENTAL SETUP

The experiments were performed on single-crystal ε-GaSe films 15–20 μm thick, so oriented that the optical axis was perpendicular to the layer. In its photoluminescent, lasing, nonlinear, and other characteristics this semiconductor is regarded as one of the most promising materials for quantum electronics (Refs. 15–20). It can be conveniently investigated and easily optically pumped, since its band gap in a direct transition is 2.02 eV (0.614 μm) (Ref. 17) and lies in the lasing range of widely used dye lasers.

A block diagram of the experimental setup for the measurement of the relaxation times is shown in Fig. 2. The master oscillator was an aluminum yttrium garnet laser with passive mode locking in polymethine dye No. 3247. One of the walls of the cell with the dye was the reflecting mirror of the cavity. After amplification (2) the frequency of the fundamental radiation was doubled by a KDP crystal (3) 4 cm thick. The second-harmonic (SH) pulses were used to pump two synchronous S-160 organic-dye lasers (ODL) (4).

The duration of the ODL pulses was determined by a system of two coupled cavities[21] inside the main cavity, which was matched to the length of the master oscillator, was placed in a dye cell whose walls formed a low-Q active nonlinear Fabry-Perot etalon. The dispersive elements were diffraction gratings with 1200 lines/mm, operating in the autocollimation regime. At a cell thickness 2 mm, the LOD generated spectrally limited pulses of 2 ps duration in a range 0.59–0.65 μm. The efficiency of conversion into tunable radiation reached 15% and the peak power was 50 kW.

The light-pulse parameters were measured by a zero-background autocorrelation procedure. Their duration was determined from the dependence of the energy of the noncollinear SH, generated in a KDP crystal 2 mm thick, on the time delay. The angle between the beams in the autocorrelator was 6°. The absence of phase modulation was monitored against the agreement between the second- and third-order autocorrelation-function (ACF) widths as determined by measuring the self-diffraction signal in the thin (20 μm) gallium-selenide film. The decay of the ACF characterizes in this case the pulse-coherence time.[22] Direct measurements of the spectrum width yielded a value $\delta\omega \sim 1.2$ cm^{-1}.

The formation of the beams needed for the measurements is clearly illustrated in Fig. 2. The time intervals between pulses was varied by delay lines 5. The angle between the wave polarizations was varied with polarization-rotators 6. All three beams were focused onto the sample 7. The useful signal was separated by spatial (8) and spectral (9) filter systems. The latter system was a diffraction grating with a period 1200 mm^{-1}, operating in second order.

The recording system included calibrated pyro- and photoreceivers 10, whose signal was filtered and processed by a DZ-28 computer (11). The dynamic range of the measurements reached seven orders and was achieved through variation of the photomultiplier sensitivity by discrete calibrated switching of the voltage supply 12. The system operated in a digital gating regime.

The measurement system had thus all the degrees of freedom needed for experimental implementation of the described measurement procedure.

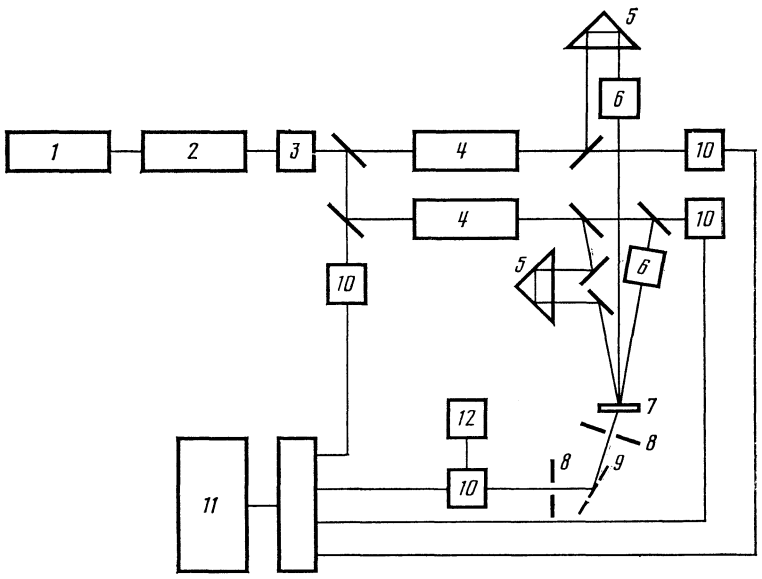

FIG. 2. Experimental setup: 1—master oscillator, 2—amplifier, 3—frequency doubler, 4—dye lasers, 5—delay lines, 6—polarization rotators, 7—sample, 8—diaphragms, 9—monochromator, 10—radiation receivers, 11—computer, 12—photomultiplier power supply.

6. BIHARMONIC-PUMPING METHOD

The experimental dependence of the scattered-field energy W_4 on the detuning $\Delta\omega_{10} = \omega_{10} - \omega_{30}$ of the central frequencies of the interacting pulses is plotted in Figs. 3a–3c for different polarizations of the interacting waves. A characteristic feature of these curves is the presence of three essentially different sections—a central peak, a pronounced gently sloping region, and an inflection point followed by a rapid descent.

The theoretical and experimental results can be compared and the times of the fast relaxation processes determined only by a painstaking stage-by-stage analysis of the various sections of all the curves. This procedure can successively single out the dominant relaxation mechanisms for each section and obviates the need for large number of adjustment parameters.It is first necessary to integrate Eq. (3) over the pump spectra. It was assumed that they are Lorentzian:

$$E_j(\omega_j) \sim [1 - i(\omega_j - \omega_{j0})/\delta\omega]^{-1}, \quad j = 1, 2, 3, \quad \omega_{10} = \omega_{20},$$

meaning an exponential pulse profile. Allowance for the finite width of the spectrum has practically no effect in the region $\Delta\omega_{10} \sim \gamma_{2,3,4}$, and at small detunings $\Delta\omega_{10} \lesssim \gamma_{1,5,6} \ll \delta\omega$, the plot of W_4 is determined indeed by the value of $\delta\omega$.

A. Parallel polarizations

In this case the $W_4(\Delta\omega_{10})$ plot differs substantially from the two following ones (Figs. 3b and 3c). At small detunings, an increase of W_4 is observed with a relative rise $\sim 10^5$ of the central peak. In the range $\Delta\omega_{10} \sim 200$–$250$ cm^{-1} the curve has a characteristic rise. It can be attributed to scattering by LO_1 optical phonons of frequency ~ 250 cm^{-1}. Polariton scattering, which was not taken into account before, turns out to be essential for the interpretation of the results. Its acoustic branch explains the course of the plot at low detunings. The acoustic-phonon lifetime is 10^{-7} s, much longer than the lasing-train duration. Owing to the pileup effect, the contribution of this type of polariton scattering should influence the measurement results particularly strongly. The individual acoustic modes, however, are not resolved,[23] since the pumps have sufficiently broad spectra.

In first-order approximation, the polariton scattering can be considered independently; this leads to an additive introduction of a Mandel'shtam-Brillouin cubic nonlinearity[14,23]:

$$\chi_{\alpha\beta\xi\eta} \sim \frac{\delta_{\alpha\beta}\delta_{\xi\eta} + \delta_{\alpha\xi}\delta_{\beta\eta}}{\Omega^2 - \Delta\omega_1^2 - 2i\gamma\Delta\omega_1}, \tag{7}$$

where $\alpha, \beta, \xi, \eta = x, y, z$; Ω and γ^{-1} are the frequency and lifetime of the acoustic phonons. For parallel polarizations, the contribution of this nonlinearity is a maximum and predominates in the vicinity of zero detuning. The presence of such a slow nonlinearity has enabled the authors of Ref. 22 to measure the field coherence function.

The initial section of the curve in Fig. 3a agrees well with the theoretical descent obtained for the Mandel'shtam-Brillouin nonlinearity (7) at a pump-spectrum width $\delta\omega = 1.08 \pm 0.10$ cm^{-1}.

B. Crossed polarizations

The case of crossed polarization of the pump waves (Fig. 3b) is much simpler to analyze. In view of the selection rules (7), polariton scattering hardly affects the measurement results. The slight rise of the curve at small detunings is due to the $\sim 2°$ error in the setting of the polarization-plane rotation angle.

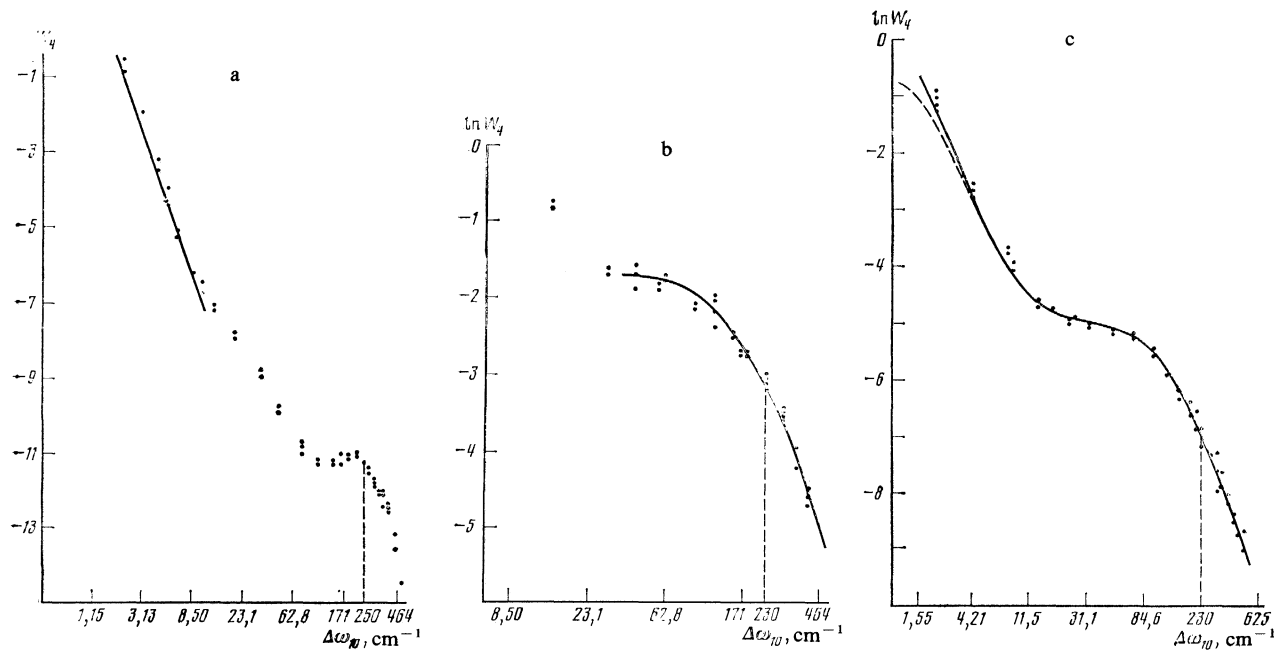

FIG. 3. Biharmonic-pumping method. Dependence of the scattered-field energy on the frequency detuning: a—parallel polarization, b—crossed polarizations, c—the angle between the polarizations is $\psi_0 = \arctan\sqrt{2}$.

At frequencies $\Delta\omega_{10} \gg \delta\omega$ the theoretical form of the curve should be described by Eq. (6). Assuming a large inhomogeneous bandwidth $2\gamma_3'/\gamma_2^* \ll 1$, the second term of this expression can be neglected. The transverse relaxation rate γ_2 is determined by the sum of the rates of all the relaxation processes,[12] so that we must put in (6)

$$\gamma_3' + \gamma_4 \approx \gamma_2. \tag{8}$$

The bringing into coincidence of the theoretical and experimental functions $W_4(\Delta\omega_{10})$ by means of only one fit parameter γ_2 (Fig. 3b) permits an unambiguous determination of the transverse relaxation rate in the sample, $\gamma_2 = 230 \pm 10$ cm^{-1}. The theoretical curves were matched to the experimental points by least squares. The error in the determination of the fit parameters is equal to twice the sum of the squares of the deviations.

C. Polarizations that eliminate the elastic orientational relaxation times

By a special choice of the angle between the pump polarizations, $\psi_0 = \arctan\sqrt{2}$, the elastic orientational relaxation time $\tilde{\gamma}_4 = \gamma_4' + D_\theta/6$ is eliminated from the expression (6) for the scattered field. A stage-by-stage matching of the calculated curve to the experimental dependences makes it possible to determine in succession the inelastic intraband relaxation rates γ_5 and $\tilde{\gamma}_4$. The rate $\tilde{\gamma}_4$ is determined with account taken of the previously obtained value $\gamma_2 = \gamma_3 + \tilde{\gamma}_4$.

For the employed gallium selenide samples of thickness 15 to 20 μm and for an angle 9.2° between the pump-propagation directions, the coefficients $C_{\alpha 11}^{(n)}$ in (6) decrease rapidly enough to permit retention of only the first of them, $C_{\alpha 11}^{(0)}$. The descent of the curve after the inflection is determined then by the first term of (6), which contains the previously obtained rate γ_2 and the only unknown quantity γ_3. The calculated curve of Fig. 3c corresponds in the region $\Delta\omega_{10} \gtrsim 50$ cm^{-1} to a value $\gamma_3 = 150 \pm 15$ cm^{-1}. According to (8), the rate of the elastic orientational relaxation is $\tilde{\gamma}_4 = 80 \pm 15$ cm^{-1}. The ratios $\gamma_3/\gamma_2 = 0.65 \pm 0.05$ and $\tilde{\gamma}_4/\gamma_2 = 0.35 \pm 0.05$ turn out to be more accurately determined.

After integration over the pump spectrum, the second term of (6) is independent of the rates of the slow relaxational processes. The theoretical expression for W_4 in the region of small detunings contains again a single unknown, $2\gamma_3/\gamma_2^*$. Variations of this parameter alter substantially the length of the gently sloping region in the region of the inflection point. The calculated curve (dashed) in Fig. 3c corresponds to a value $2\gamma_3/\gamma_2^* = (4.2 \pm 0.2)\cdot 10^{-2}$ and determines $\gamma_2^* = (6.7 \pm 0.5)\cdot 10^3$, thus confirming the initial assumption that the electronic transition is essentially inhomogeneous.

At the chosen pump-wave polarizations, scattering of acoustic phonons should occur and explain the negligible deviation of the calculated position of the central peak from the experimental one. The solid curve of Fig. 3c corresponds to additive allowance for the contribution of the Mandel'sh-

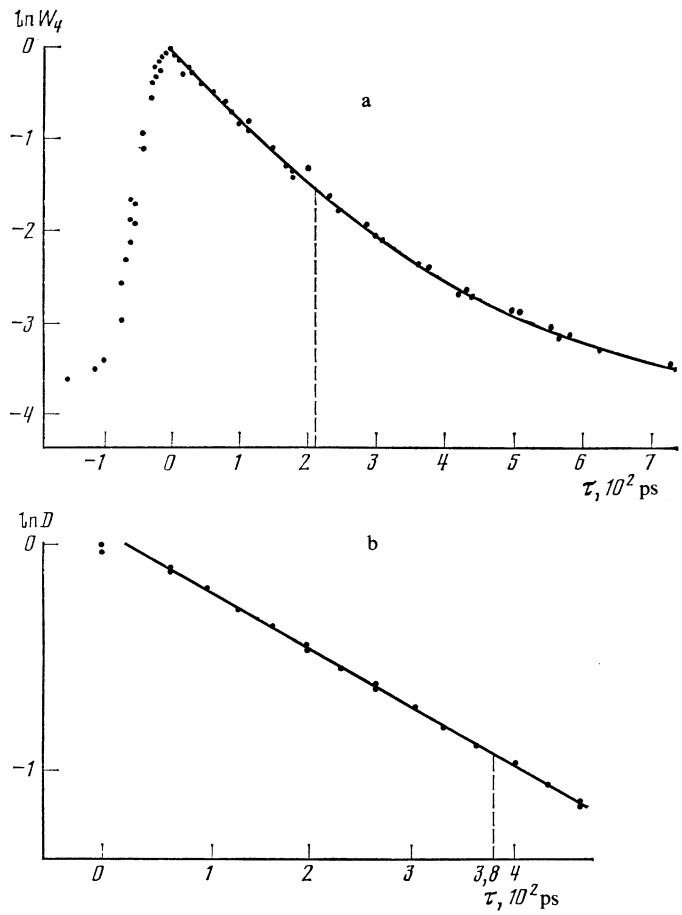

FIG. 4. Probing-beam method. Dependence of the scattered-field energy (a) and of the sample optical density $D(\tau)$ (b) on the pulse delay time.

tam-Brillouin nonlinearity (7) with a relative weight $(8 \pm 2) \lesssim 10^{-4}$.

7. PROBING-BEAM METHOD

In the measurements of the group of slow relaxation times (4) the scattered field is determined by Eq. (5), in which it suffices as before to retain only the first term of the sum, with $n = 0$.

The experimental dependence of the scattered-field energy $W_4(\tau)$ on the delay time between the pulses is shown in Fig. 4a. The angle between the pumping beams $E_{1,3}$ was $(9.2 \pm 0.2)°$. The measurments were made at a small frequency difference between the interacting waves, $\omega_{20} - \omega_{10,30} = 10\ \text{cm}^{-1}$. The signal-wave propagation direction did not coincide with the bisector of the angle between the pump beams. The measures taken made it possible to avoid the permutation $i \leftrightarrow j$ in Eq. (3), and as a result W_4 did not have a sharp peak in the region $\tau \lesssim \tau_p$ where all three pulses crossed.[24]

Scattering by the grating of the long-lived acoustic phonons and pileup along the train lowered substantially the measurement contrast. Its contribution to the scattered-field amplitude during the relaxation times of the electronic nonlinearity is reduced to allowance for an additive and practically constant background in (5). The background level can be determined from the value of W_4 in the region $\tau < -\tau_p < 0$. Subsequent "subtraction" of the background yields the effective relaxation rate of the electronic nonlinearity:

$$\gamma_{\text{eff}} = \gamma_1 + \gamma_5 = (4.69 \pm 0.21) \cdot 10^9\ \text{s}^{-1}. \quad (9)$$

Similar measurement were made for an angle $(6.8 \pm 0.2)°$ between the pump beams. However, this method of identifying the contributions of the longitudinal relaxation and of the spatial diffusion[1] is of low accuracy in the case of gallium selenide, since the characteristic time of the first process is quite small.[17] For this reason, γ_1 was determined directly by measuring the dependence of the optical density of the sample on the probing-pulse delay time.[4] The results are shown in Fig. 4b. The rate of interband relaxation was $\gamma_1 = (2.63 \pm 0.14) \cdot 10^9\ \text{s}^{-1}$, corresponding to a spatial-diffusion coefficient [Eq. (2)] $D_r = 7.5 \pm 1.4\ \text{cm}^2/\text{s}$.

8. CONCLUSION

It must be noted that in rough limiting cases the theoretical results of this paper agree with relations obtained earlier by many workers.[1-7] At the same time, they explain a number of "anomalies"observed in the behavior of the nonlinear response, refine the interpretation of the measured quantities, and indicate the limits of applicability of the models.

An optimal combination of the methods of biharmonic pumping and probing beam has made it possible, within the framework of a phenomenological theory, to measure and identify the times of the following relaxation processes in ε-GaSe: transverse relaxation ($T_2 = 23.1 \pm 1.6$ fs), inelastic intraband relaxation ($T_3 = (35.8 \pm 4.0$ fs), elastic orientational relaxation ($T_4 = 69 \pm 13$ fs), interband relaxation ($T_1 = 380 \pm 20$ ps), and transverse spatial diffusion ($T_5 = 490 \pm 80$ ps); the latter corresponds to a spatial diffusion coefficient $D_r = 7.5 \pm 1.4\ \text{cm}^2/\text{s}$.

The experimental investigations reported confirm the validity of the theoretical analysis based on a phenomenological description of the relaxation processes. The results can be interpreted without resorting to the theory of non-Markov processes.[10,11]

The authors thank S. A. Akhmanov and V. T. Platonenoko for helpful discussions.

[1]A. L. Smirl, Dynamics of High-Density Transient Electron-Hole Plasmas in Germanium, Preprint, Academic Press, 1983.
[2]T. E. Bogges, A. L. Smirl, and B. S. Wherret, Opt. Commun. **43**, 128 (1982).
[3]T. Yajima and Y. Taira, J. Phys. Soc. Jpn. **47**, 1620 (1979).
[4]H. E. Lessing and A. von Jena, Chemical Phys. Lett. **42**, 213 (1976).
[5]T. Yajima and H. Souma, Phys. Rev. **A17**, 309, 324 (1978).
[6]J. J. Song, J. H. Lee, and M. D. Levenson, Phys. Rev. **A17**, 1439 (1978).
[7]S. Y. Yuen and P. A. Wolff, Appl. Phys. Lett. **40**, 457 (1982).
[8]M. A. Vasil'eva, V. I. Malyshev, and A. V. Masalov, Kratk. soobshch. fiz. FIAN No. 1, 35 (1980).
[9]V. L. Vinetskiĭ and N. V. Kukharev, Kvant. Elektron. (Moscow) **4**, 420 (1977) [Sov. J. Quant. Electron. **7**, 230 (1977)].
[10]B. D. Fainberg, Opt. Spetrosk. **55**, 1098 (1983).
[11]M. Aihara, Phys. Rev. **B25**, 53 (1982).
[12]P. A. Apanasevich, Osnovy teorii vzaimodeĭstviya sveta s veshchestvom (Principles of the Theory of Interaction of Light with Matter), Minsk, Nauka i tekhnika, 1977.
[13]A. I. Ansel'm, Vvedenie v teoriyu poluprovodnikov (Introduction to Semiconductor Theory), Nauka, 1978.
[14]S. A. Akhmanov and I. M. Koroteev, Metody nelineĭnoĭ optiki v spektroskopii rasseyaniya sveta (Methods of Nonlinear Optics in Light-Scattering Spectroscopy), Nauka, 1981.
[15]Z. S. Medvedeva, Khal'kogenidi elementov 3B podgruppy periodicheskoĭ sistemy (Chalcogenides of Elements of the 3B Subgroup of the Periodic Table), Nauka, 1968.
[16]V. V. Sobolev, Zony i éksitony khal'gogenidov galliya, indiya, i talliya (Bands and Excitons of the Chalgogenides of Gallium, Indium, and Thallium), Kishinev, Shtinitsa, 1982.
[17]S. S. Yao, J. Buchert, and R. R. Alfano, Phys. Rev. **B25**, 6534 (1982).
[18]J. L. Staehli and A. Frova, Physica (Utrecht) **99B**, 299 1980).
[19]V. Angelli, C. Manfredotti, R. Murri, and L. Vasanelli, Phys. Rev. **B17**, 3221 (1978).
[20]R. Baltramejunas, G. Guseinov, V. Varkevičius, V. Niunka, J. Vaitkus, and J. Viščakas, Opt. Commun. **11**, 274 (1974).
[21]K. D. Egorov, V. M. Petnikova, S. A. Pleshanov, and V. V. Shuvalov, Kvant. Electron. (Moscow) **12**, 44 (1984) [*sic*].
[22]R. Baltrameyunas, Yu. Vaĭtkus, R. Daneliyus, M. Pyatrauskas, and A. Piskarskas, *ibid.* **9**, 1921 (1982) [**12**, 1252 (1982)].
[23]N. I. Koroteev and M. F. Ternovskaya, *ibid.* **9**, 1967 (1982) [**12**, 1281 (1982)].
[24]D. Reiser and A. Laubereau, Opt. Commun. **42**, 329 (1982).

Translated by J. G. Adashko